

LC-PHSM-2003-016

June 16, 2003

Measuring the Luminosity of a $\gamma\gamma$ Collider with $\gamma\gamma \rightarrow \ell^+\ell^-\gamma$ Events

V. Makarenko

NC PHEP BSU

E-mail: makarenko@hep.by

K. Mönig

DESY, Zeuthen

E-mail: klaus.moenig@desy.de

T. Shishkina

NC PHEP BSU

E-mail: shishkina@hep.by

Abstract. The process $\gamma\gamma \rightarrow \ell^+\ell^-$ is highly suppressed when the total angular momentum of the two colliding photons is zero so that it cannot be used for luminosity determination. This configuration, however is needed for Higgs production at a photon collider. It will be shown that the process $\gamma\gamma \rightarrow \ell^+\ell^-\gamma$ can be used in this case to measure the luminosity of a collider with a precision that is good enough not to limit the error on the partial decay width $\Gamma(H \rightarrow \gamma\gamma)$.

1. Introduction

Linear lepton colliders will provide the possibility to investigate photon collisions at energies and luminosities close to those in e^+e^- collisions [1]. If a light Higgs exists one of the main tasks of a photon collider will be the measurement of the partial width $\Gamma(H \rightarrow \gamma\gamma)$ [2]. Not to be limited by the error from the luminosity determination the luminosity of the collider at the energy of the Higgs mass has to be known with a precision of around 1%. To produce scalar Higgses the total angular momentum of the two photons has to be $J = 0$. In this case the cross section $\gamma\gamma \rightarrow \ell^+\ell^-$ is suppressed by a factor m_ℓ^2/s and thus not usable for luminosity determination. The radiative process $\gamma\gamma \rightarrow \ell^+\ell^-\gamma$ is suppressed by an additional factor α , however due to the additional final state photon the spin suppression does no longer apply. It is therefore worth examining if the radiative process can be used for luminosity determination.

For this reason we consider the exclusive reaction $\gamma\gamma \rightarrow \ell^+\ell^-\gamma$ as a possible candidate for a calibration channel at a photon collider.

The two helicity configurations of the $\gamma\gamma$ -system lead to different spectra of the final state particles. We have analysed the behaviour of the $\gamma\gamma \rightarrow \ell^+\ell^-\gamma$ reaction for the various helicities of the beam as a function of different observables. Since the photon beams in the collider are only partially polarised the ratio of the cross sections of $\gamma\gamma \rightarrow \ell^+\ell^-\gamma$ scattering for $J = 0$ to $J = 2$ -beams should be high for the luminosity measurement. The main emphasis of this analysis is put on $\sqrt{s} = 120$ GeV, which is about the mass, where a light Higgs boson is expected.

2. Cross sections of $\gamma\gamma \rightarrow \ell^+\ell^-\gamma$

We consider the process

$$\gamma(p_1, \lambda_1) + \gamma(p_2, \lambda_2) \rightarrow f(p_1', e_1') + \bar{f}(p_2', e_2') + \gamma(p_3, \lambda_3), \quad (1)$$

where λ_i and e_i' are photon and fermion helicities.

The centre of mass energy squared is denoted by $s = (p_1 + p_2)^2 = 2p_1 \cdot p_2$, and the final-state photon energy by $\omega = p_3$. For the differential cross-section we introduce the normalised final-state photon energy (c.m.s. is used) $x = w/\sqrt{s}$. The total helicity of the $\gamma\gamma$ system is denoted by $J = |\lambda_1 - \lambda_2|$.

We consider the cross section

$$\sigma = \int \frac{1}{2s} |M(\lambda_1, \lambda_2, e_1', e_2', \lambda_3)|^2 d\Gamma,$$

where the phase-space volume element is defined by

$$d\Gamma = \frac{d^3p_1'}{(2\pi)^3 2p_1'^0} \cdot \frac{d^3p_2'}{(2\pi)^3 2p_2'^0} \cdot \frac{d^3p_3}{(2\pi)^3 2p_3^0} \cdot (2\pi)^4 \delta(p_1 + p_2 - p_1' - p_2' - p_3).$$

The process $\gamma\gamma \rightarrow \ell^+\ell^-\gamma$ is in Born approximation a pure QED reaction. The contributing Feynman diagrams are shown in figure 1. Using the method of helicity amplitudes [3], the squared matrix elements are obtained [4]:

$$|M^{+---++}|^2 = 4e^6 \frac{p_1' \cdot p_2' (p_2' \cdot p_2)^2}{p_1' \cdot p_3 p_2' \cdot p_3 p_1' \cdot p_1 p_2' \cdot p_1}. \quad (2)$$

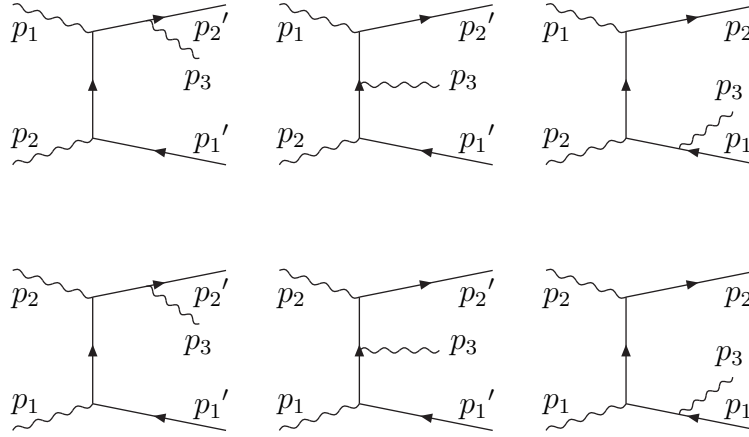


Fig. 1. Diagrams for the process $\gamma\gamma \rightarrow \ell^+\ell^-\gamma$.

All other non-vanishing amplitudes are obtained from $|M^{+---++}|$ by using C, P, Bose and crossing (between final and initial particles) symmetries:

$$\begin{aligned}
 d\sigma^{+---} &= d\sigma^{+---++}|_{1 \leftrightarrow 2}, \text{ (P + Bose)} \\
 d\sigma^{+--+} &= d\sigma^{+---++}|_{1' \leftrightarrow 2'}, \text{ (C)} \\
 d\sigma^{+--+} &= d\sigma^{+---++}|_{1 \leftrightarrow 2, 1' \leftrightarrow 2'}, \text{ (CP + Bose)} \\
 d\sigma^{++--} &= d\sigma^{+---++}|_{1 \leftrightarrow 2, 1' \leftrightarrow 2'}, \text{ (C + crossing)} \\
 d\sigma^{++--} &= d\sigma^{+---++}|_{1' \leftrightarrow 2'}, \text{ (C)} \\
 d\sigma^{-\lambda_1, -\lambda_2, -e_1', -e_2', -\lambda_3} &= d\sigma^{\lambda_1, \lambda_2, e_1', e_2', \lambda_3}. \text{ (P)}
 \end{aligned}$$

Since final-state polarisations cannot be measured we sum over all final particle helicities. The further integration is performed numerically using a Monte-Carlo method [5].

3. Comparison of $J=0$ and $J=2$ contributions

Calculations for various experimental restrictions on the parameters of final particles have been performed. The events are not detected if energies and angles are below the corresponding threshold values. The considered cuts on the phase-space of final particles are denoted as follows:

- Minimum final-state photon energy: ω_{min} ,
- Minimum fermion energy: $E_{\ell, min}$,
- Minimum angle between any final and any initial state particle (polar angle cut): Θ_{min} ,
- Minimum angle between any pair of final state particles: φ_{min} .

In figures 2 and 3 the photon energy spectra for the beam polarisations $J=0$ and $J=2$ at various cuts are presented. The differential cross section $d\sigma/dx$ for $J=2$ beams decreases while the one for $J=0$ beams rises with increasing final-state photon energy.

In fig. 4 we show the total cross section dependence on the ω -cut and the ratio $\sigma_{J=0}/\sigma_{J=2}$.

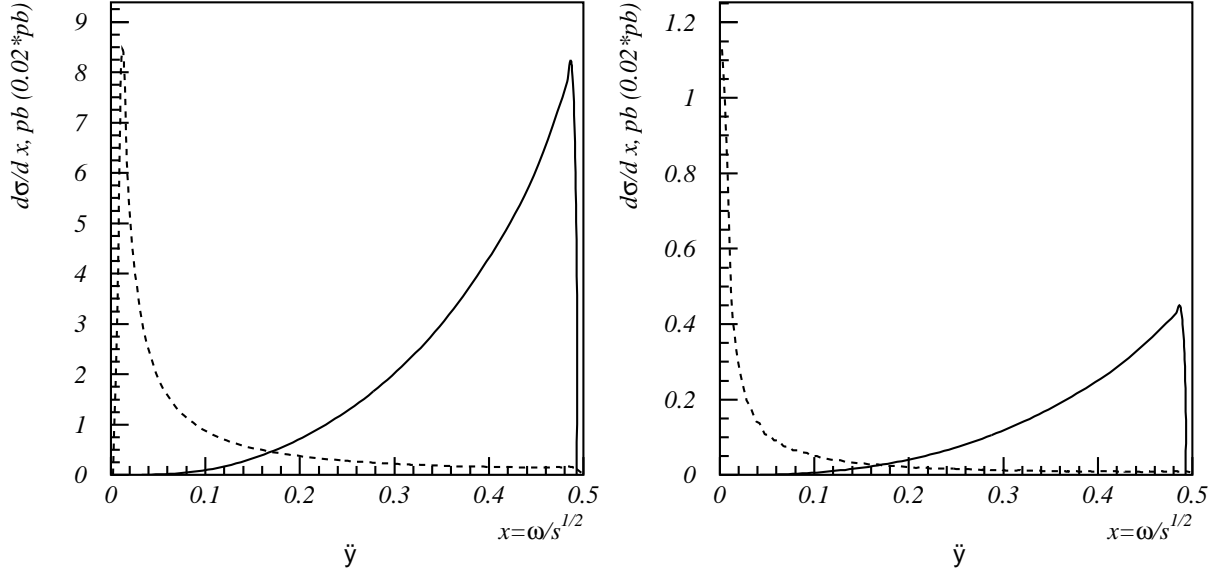


Fig. 2. Final-state photon energy spectrum for $J=0$ (dotted) and $J=2$ (solid) at $\sqrt{s} = 120$ GeV (left) and $\sqrt{s} = 500$ GeV (right). Cuts: $\Theta_{min} = 7^\circ$, $\varphi_{min} = 3^\circ$, $E_{\ell,min} = 1$ GeV, $\omega_{min} = 1$ GeV. The $J=2$ cross section has been multiplied by 0.02.

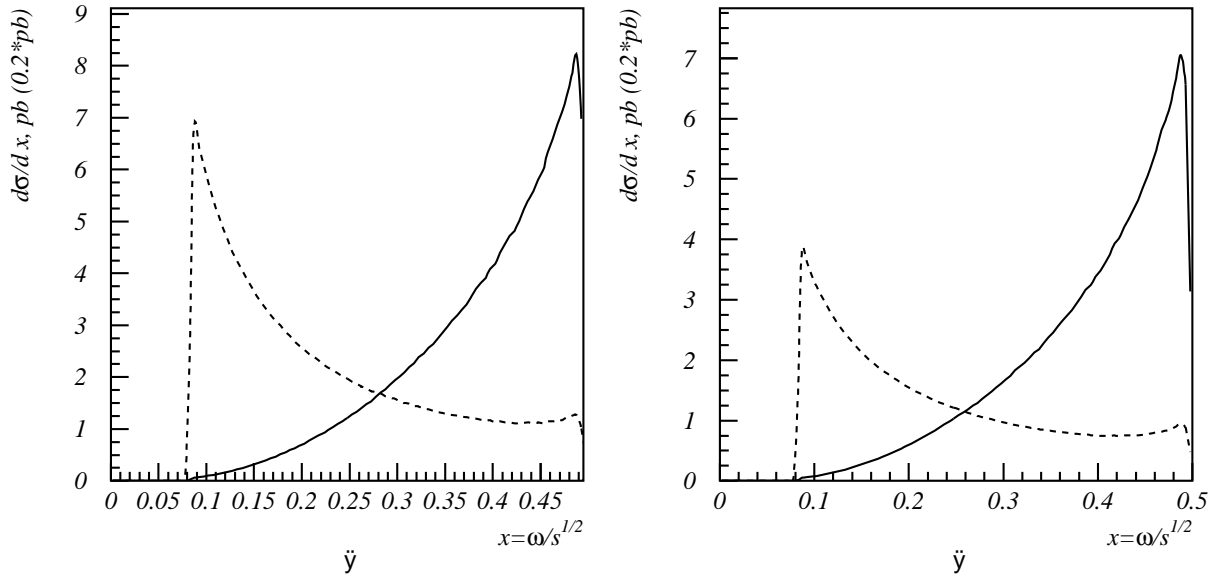


Fig. 3. Final-state photon energy spectrum for $J=0$ (solid) and $J=2$ (dotted) at $\sqrt{s} = 120$ GeV. Cuts: $\Theta_{min} = 7^\circ$, $\varphi_{min} = 10^\circ$ (left) and $\varphi_{min} = 30^\circ$ (right), $E_{\ell,min} = 1$ GeV, $\omega_{min} = 10$ GeV. The $J=2$ cross section has been multiplied by 0.2.

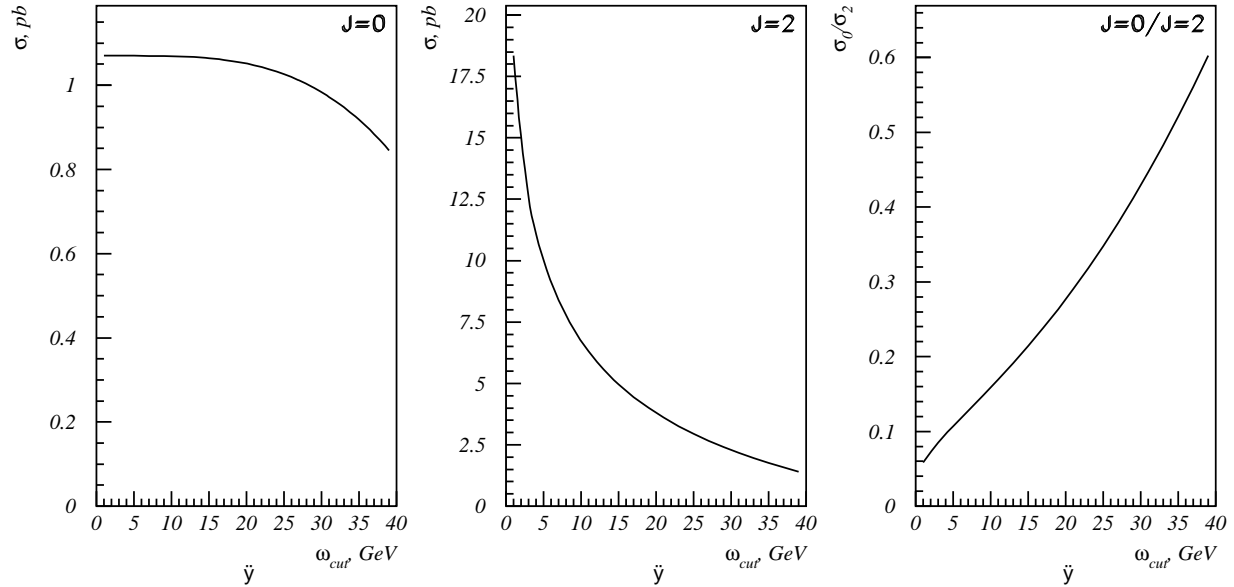


Fig. 4. Cross sections for $\omega > \omega_{min}$ for $J=0$ and $J=2$ and their ratio.

A ratio $\sigma_{J=0}/\sigma_{J=2} > 0.5$ can be achieved without a large loss in $\sigma_{J=2}$.

In figure 5 the minimum angle between the photon and one of the two leptons, φ , is shown for both beam polarisations. As already shown for the photon energy for $J = 2$ one can see the typical final state radiation pattern with the colinear and infrared divergencies while for $J = 0$ large angles are preferred. The total cross sections with $\varphi > \varphi_{min}$ for $J = 0$ and $J = 2$ and their ratio are shown in figure 6.

Figure 7 shows the two total cross sections and their ratio as a function of Θ_{min} . It is interesting to note that a low cut on Θ is not only needed to get a large cross section but also enhances the $J = 0$ component.

The total cross section dependence on the centre of mass energy is shown in figure 8. It follows very well a $1/s$ distribution.

All results presented in this section agree with an independent analysis using Whizard [6]. For $\sqrt{s} = 400$ GeV the results agree also with a calculation using CompHEP [7].

4. Luminosity measurement

The final cuts have been chosen to be

$$\begin{aligned}\Theta_{min} &= 7^\circ, \\ \omega_{min} &= 20 \text{ GeV}, \\ E_{\ell,min} &= 5 \text{ GeV}, \\ \varphi_{min} &= 30^\circ.\end{aligned}$$

These cuts simultaneously enhance the $J = 0$ cross section compared to the $J = 2$ one and ensure that the events can be identified cleanly with the detector. With these cuts the final cross sections are

$$\begin{aligned}\sigma(J = 0) &= 0.82 \text{ pb} \\ \sigma(J = 2) &= 1.89 \text{ pb}\end{aligned}$$

For the standard beam and laser parameters the fraction of the $J = 0$ polarisation in the total luminosity is of the order 95% so that the selected $\gamma\gamma \rightarrow \ell^+\ell^-\gamma$ sample has a purity

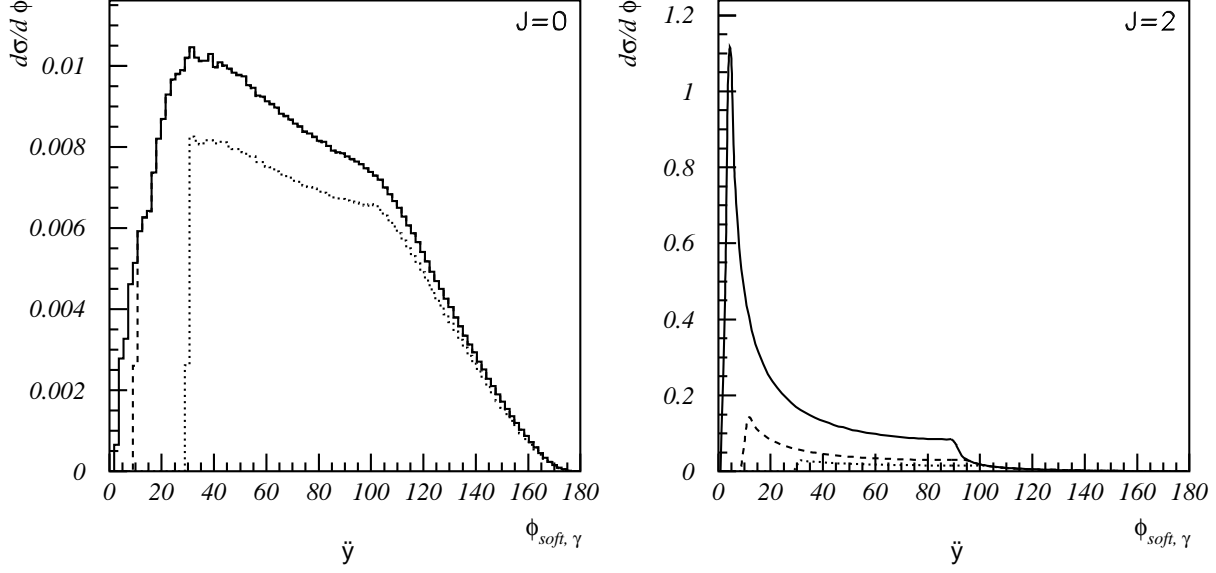


Fig. 5. $d\sigma/d\varphi$ at $\sqrt{s} = 120$ GeV for $J = 0$ and $J = 2$ and various cuts: $\Theta_{min} = 7^\circ$, $\varphi_{min} = 3^\circ$, $E_{\ell,min} = 1$ GeV, $\omega_{min} = 1$ GeV (solid line); $\Theta_{min} = 7^\circ$, $\varphi_{min} = 10^\circ$, $E_{\ell,min} = 1$ GeV, $\omega_{min} = 10$ GeV (dashed line); $\Theta_{min} = 7^\circ$, $\varphi_{min} = 30^\circ$, $E_{\ell,min} = 5$ GeV, $\omega_{min} = 20$ GeV (dotted line).

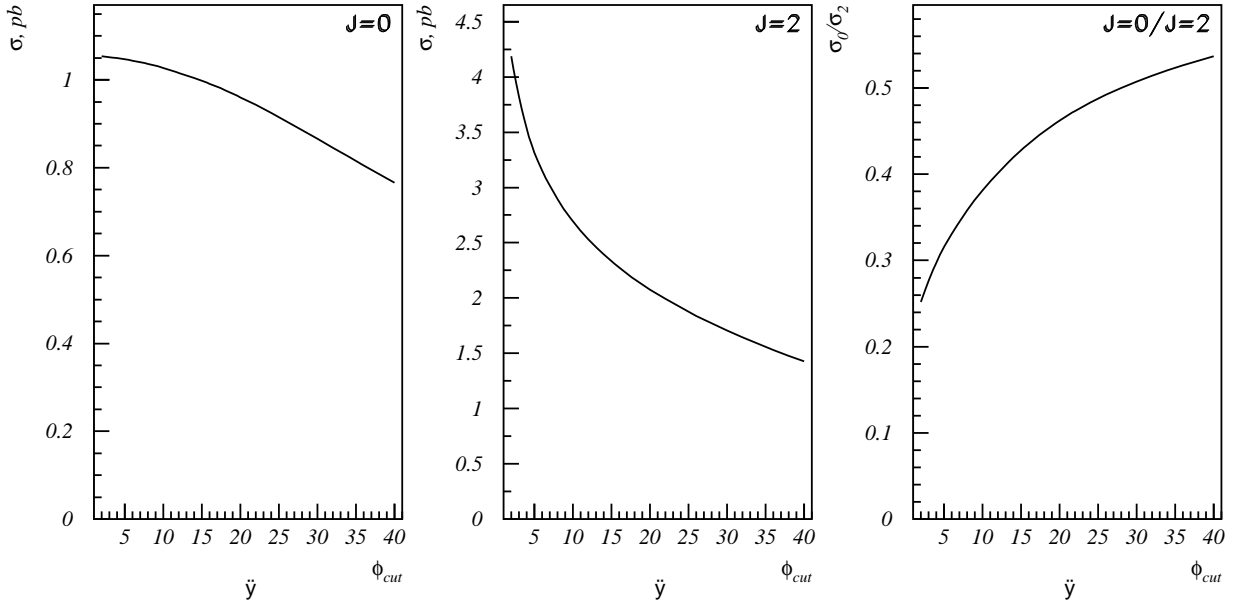


Fig. 6. Cross sections for $\varphi > \varphi_{min}$ for $J=0$ and $J=2$ and their ratio.

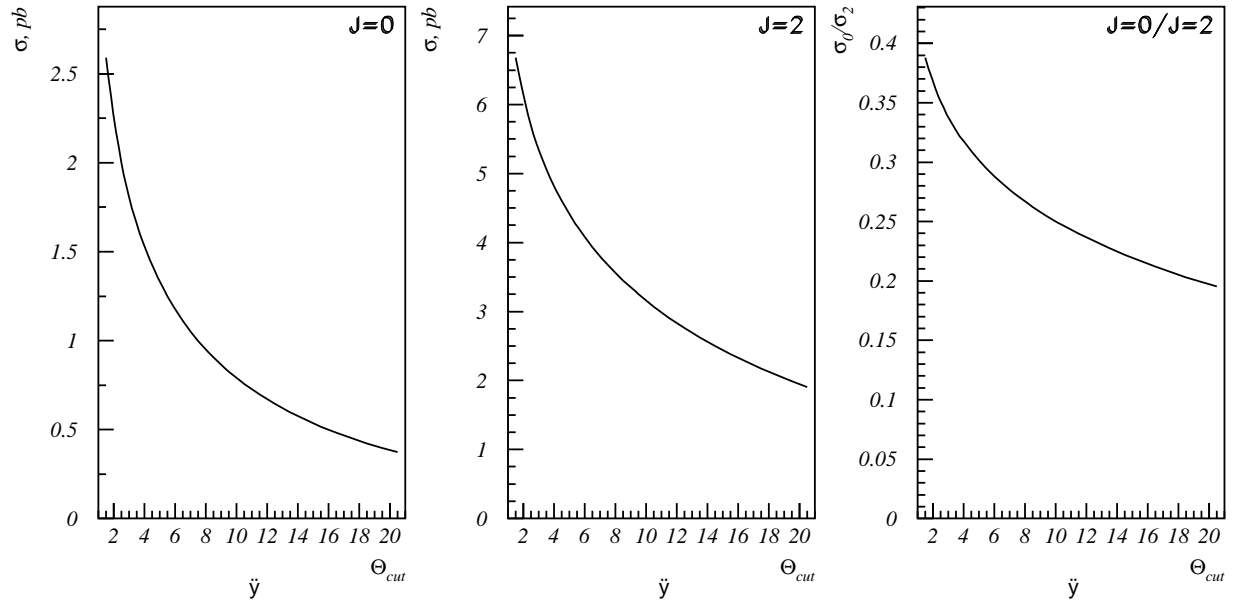


Fig. 7. Cross sections for $\Theta > \Theta_{min}$ for $J=0$ and $J=2$ and their ratio.

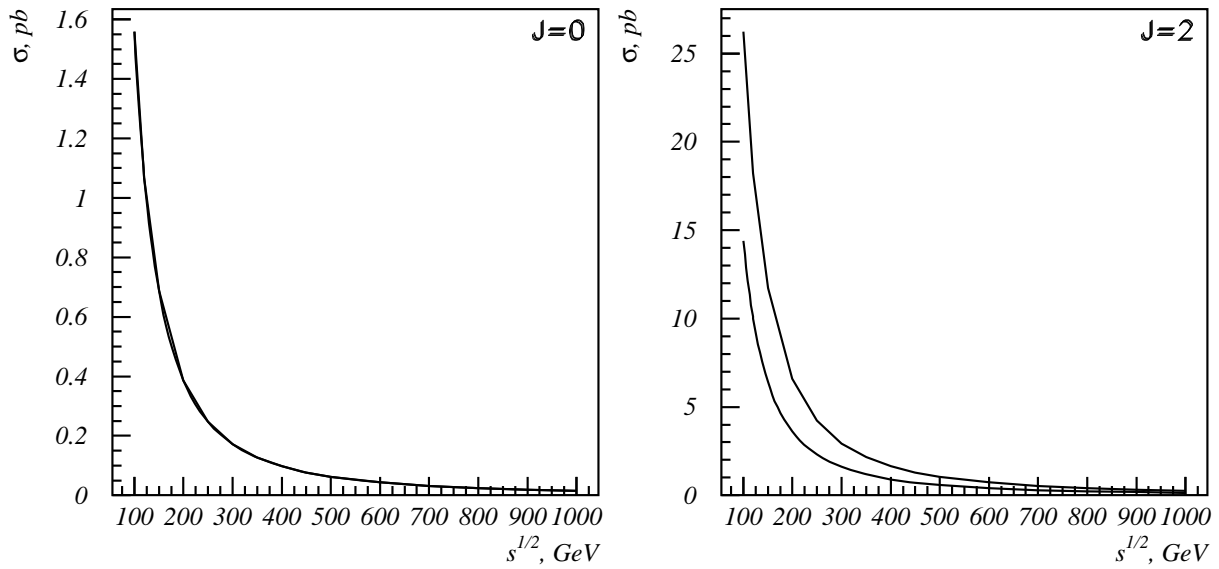


Fig. 8. The dependence of the total cross section on \sqrt{s} . The cuts are: $\Theta_{min} = 7^\circ$, $\varphi_{min} = 3^\circ$, $E_{\ell,min} = 1 \text{ GeV}$, $\omega_{min} = 1 \text{ GeV} \cdot (\sqrt{s}/120 \text{ GeV})$ (upper line) and $\omega_{min} = 5 \text{ GeV} \cdot (\sqrt{s}/120 \text{ GeV})$ (lower line).

of around 90%. The $J = 2$ background can be measured accurately with $\gamma\gamma \rightarrow \ell^+\ell^-$ events. For an electron beam energy of $E_e = 100$ GeV the TESLA design luminosity for the high energy part of the beam is $\mathcal{L}(\sqrt{s'} > 0.8\sqrt{s'_{\max}}) = 4.8 \cdot 10^{33} \text{cm}^{-2}\text{s}^{-1}$ and for a window of ± 2 GeV around a Higgs mass of 120 GeV it is $\mathcal{L}(m_H \pm 2 \text{ GeV}) = 7 \cdot 10^{32} \text{cm}^{-2}\text{s}^{-1}$ [2, 8]. In a two year run ($2 \cdot 10^7 \text{s}$) using muons only this leads to a statistical precision on the luminosity measurement of

$$\begin{aligned} \frac{\Delta\mathcal{L}}{\mathcal{L}} \left(\sqrt{s'} > 0.8\sqrt{s'_{\max}} \right) &= 0.4\% \\ \frac{\Delta\mathcal{L}}{\mathcal{L}} (m_H \pm 2 \text{ GeV}) &= 1.0\%. \end{aligned}$$

Adding electrons these precisions improve by a factor $1/\sqrt{2}$.

The size of the mass window around m_H that can be used for luminosity determination depends on the confidence one has in the luminosity spectrum once the data are available. Studies with Circe2 [9] and Cain [8] indicate that the differential luminosity in a 2 GeV window around the maximum changes by less than 1% so that this window is certainly safe. Studies with the fast simulation program Simdet [10] show that the invariant mass resolution of the detector for the accepted events is around 1 GeV, consistent with a 2 GeV mass window.

5. Conclusions

The differential luminosity of a photon collider running with $J = 0$ at a $\gamma\gamma$ -centre of mass energy around 120 GeV to produce light Higgses can be measured with an accuracy around 0.7% in a two years run. The uncertainty of the event rate $\gamma\gamma \rightarrow H \rightarrow b\bar{b}$ in the same running time will be around 1.5% [11, 12] and the one of the branching ratio $\text{BR}(H \rightarrow b\bar{b})$ from e^+e^- running will be around 2.5% [13], so that the uncertainty on the partial width $\Gamma(H \rightarrow \gamma\gamma)$ will not be limited by the error on the luminosity.

References

- [1] I.F. Ginzburg, G.L. Kotkin, V.G. Serbo and V.I. Telnov, Nucl. Instr. Meth. **205** (1983) 47;
I.F. Ginzburg, G.L. Kotkin, S.L. Panfil, V.G. Serbo and V.I. Telnov, Nucl. Instr. Meth. **219** (1984) 5.
- [2] B. Badelek *et al.*, *TESLA Technical Design Report Part VI: The Photon Collider at TESLA*, DESY-01-011E.
- [3] P. De Causmaecker, R. Gastmans, W. Troost, Tai Tsun Wu, Phys. Lett. **B105** (1981) 215;
P. De Causmaecker, R. Gastmans, W. Troost, Tai Tsun Wu, Nucl. Phys. **B206** (1982) 53;
F.A. Berends *et al.*, Nucl. Phys. **B206** (1982) 61;
S. Dittmaier, Phys. Rev. **D59** (1999) 016007, hep-ph/9805445.
- [4] T.V. Shishkina, V.V. Makarenko, hep-ph/0212409.
- [5] S. Weinzierl, NIKHEF-00-012, hep-ph/0006269.
- [6] W. Kilian, *WHIZARD 1.11 A generic Monte-Carlo integration and event generator package for multi-particle processes*, LC-TOOL-2001-039.
- [7] A. V. Pak, D. V. Pavluchenko, S. S. Petrosyan, V. G. Serbo and V. I. Telnov, hep-ex/0301037.
- [8] K. Yokoya *CAIN Version 2.35*, <ftp://lcdev.kek.jp/pub/Yokoya/cain235>
- [9] T. Ohl, *Circe Version 2.0: Beam Spectra for Simulating Linear Collider and Photon Collider Physics*, <ftp://hep1ix.ikp.physik.tu-darmstadt.de/pub/ohl/circe2/doc/manual.pdf>

- [10] M. Pohl, H. J. Schreiber, *SIMDET - Version 4, A Parametric Monte Carlo for a TESLA Detector*, DESY 02-061.
- [11] P. Niezurawski, talk at the The 4th ECFA/DESY Workshop on Physics and Detectors for a 90-800 GeV Linear e^+e^- Collider, Amsterdam, April 2003,
<http://www.nikhef.nl/ecfa-desy/ECspecific/Program/Presentations/April-2/Par-1/1A/niezurawski-p.pdf>
- [12] A. Rosca, talk at the The 4th ECFA/DESY Workshop on Physics and Detectors for a 90-800 GeV Linear e^+e^- Collider, Amsterdam, April 2003,
<http://www.nikhef.nl/ecfa-desy/ECspecific/Program/Presentations/April-2/Par-1/1A/rosca-a.ppt>
- [13] J. A. Aguilar-Saavedra et al., *TESLA Technical Design Report Part III: Physics at an e^+e^- Linear Collider*, DESY-01-011C.